



Interoperable solutions for implementing holistic **FLEXi**bility
services in the distribution **GRID**

Development of Physical Architecture

Deliverable 3.7

WP3

Grant agreement: 864579
From 1st October 2019 to 30th September 2023

Prepared by: ZIV

Date: 01/03/2022



This project has received funding from the European Union 's Horizon 2020 research and innovation programme under service agreement No 864579

Disclaimer: The sole responsibility for any error or omissions lies with the editor. The content does not necessarily reflect the opinion of the European Commission. The European Commission is also not responsible for any use that may be made of the information contained herein

DELIVERABLE FACTSHEET

Deliverable no.	D3.7
Responsible Partner	ZIV
WP no. and title	WP3 Development of Physical Architecture
Version	V2.0
Version Date	28/02/2022

Dissemination level	
X	PU → Public
	PP → Restricted to other programme participants (including the EC)
	RE → Restricted to a group specified by the consortium (including the EC)
	CO → Confidential, only for members of the consortium (including the EC)

Approvals

	Company
Author/s	ZIV, CIRCE, VIESGO, VERD, HEP-ODS, EDYNA, OP&A, SELTA, ATOS, IOSA, UNICAN, UNIZG-FER
Task Leader	ZIV
WP Leader	ZIV

Documents History

Revision	Date	Main Modification	Author
0	10/02/2022	Initial version	ZIV
1	18/02/2022	1 st review	VERD
2	28/02/2022	Final version	ZIV, CIRCE



ABBREVIATIONS

AMR. Automatic Meter Reading

DER. Distributed Energy Resources

DSO. Distribution System Operators

EB. Energy Box.

LV. Low Voltage.

LVB. Low Voltage Board.

MV. Medium Voltage

OLTC. On Load Tap Changer

PLC. Power Line Communications.

NBIoT. NarrowBand Internet of Things.

OPEX. Operational Expenditures.

RTU. Remote Terminal Unit

TOU. Time of Use

DISCLAIMER OF WARRANTIES

“This project has received funding from the European Union’s Horizon 2020 research and innovation programme under Grant Agreement No 864579”.

This document has been prepared by FLEXIGRID project partners as an account of work carried out within the framework of the EC-GA contract no 864579.

Neither Project Coordinator, nor any signatory party of FLEXIGRID Project Consortium Agreement, nor any person acting on behalf of any of them:

- (a) makes any warranty or representation whatsoever, express, or implied,
 - (i). with respect to the use of any information, apparatus, method, process, or similar item disclosed in this document, including merchantability and fitness for a particular purpose, or
 - (ii). that such use does not infringe on or interfere with privately owned rights, including any party's intellectual property, or
 - (iii). that this document is suitable to any particular user's circumstance; or
- (b) assumes responsibility for any damages or other liability whatsoever (including any consequential damages, even if Project Coordinator or any representative of a signatory party of the FLEXIGRID Project Consortium Agreement, has been advised of the possibility of such damages) resulting from your selection or use of this document or any information, apparatus, method, process, or similar item disclosed in this document.

TABLE OF CONTENTS

ABBREVIATIONS	3
DISCLAIMER OF WARRANTIES.....	4
TABLE OF CONTENTS.....	5
EXECUTIVE SUMMARY	6
1. INTRODUCTION	9
2. TASK 3.1. RESULTS AND CONCLUSIONS	10
3. TASK 3.2. RESULTS AND CONCLUSIONS	13
4. TASK 3.3. RESULTS AND CONCLUSIONS	16
5. TASK 3.4. RESULTS AND CONCLUSIONS	18
5.1 Grid Model.....	18
5.2 Scenarios and study cases	18
5.3 Main conclusions from the test results performed on the conventional feeder relay	19
5.4 Grid code and negative-sequence current injection	20
5.5 Solutions developed	20
6. TASK 3.5. RESULTS AND CONCLUSIONS	23
6.1 Behaviour of type 4 wind and PV generators.....	23
6.2 Behaviour of type 3 wind generator.....	23
6.3 Sequence networks with converter-based generation	23
6.4 New developments implemented on feeder relay IRF model and on fault passage indicator TCA model.....	23
6.5 Additional SIMULINK model	26
6.6 Testing of algorithm improvements with RTDS model results.....	27
6.7 Testing of algorithms improvements on SIMULINK model results	30
7. CONCLUSIONS	33

EXECUTIVE SUMMARY

New solutions have been specified, designed and developed in the context of FLEXIGRID project, to improve the distribution grid operation making it more flexible, reliable and cost-efficient. These solutions will allow the implementation of services currently unfeasible due to technical restrictions.

This deliverable contains all the publishable results and conclusions on the physical architecture developments obtained during the whole duration of WP3.

Secondary substation (SS) of the future, developed in T3.1, consists of a secondary substation including upgraded automation and remote metering capabilities, fault detection and advanced meter infrastructure. It will improve energy balance, energy metering, safety and efficiency, enabling to transform the classical LV distribution switchgear, with workers' safety and assets protection as main features, into a smart LV switchgear and control gear assembly with advanced functionalities ready for future network challenges. Furthermore, this SS includes the development of a new compact smart distribution transformer, with an On-Load Tap Changer (OLTC), able to regulate the voltage automatically to cope with the fluctuations generated by new loads and variable DG in the LV grid, while compensates voltages instabilities in the MV network.

The new AMI systems will pay greater attention to the needs of an increasingly informed and "digital" consumer, while reducing the OPEX for distribution companies through an innovative mechanism allowing the identification of the LV feeders of all the connected smart meters. This new generation of smart meters will count with an interface to provide real-time information to the users about their electricity demand, and act accordingly.

For the development of the new meter platform designed and developed in T3.2 by ZIV, flexibility has been considered as the main requirement, especially with regards to communications technology. The smart meter shall provide data not only to the DSO but also to end consumers or prosumers. In each market, communications technology does not have to be the same, therefore the more interfaces and more modularity we have, the more prepared we will be to adapt to new markets and technological changes. With this requirement and other less impactful ones (new records, new anti-fraud measures, etc.).

On the other hand, an improved mechanism to obtain the LV feeder identification of all the connected smart electricity meters has been developed and tested in simulation. Simulation tests have shown that the method appears to have promising results.

The Energy Box is a solution for Smart Grid and micro-grid management developed by CIRCE in T3.3. It is a multi-purpose concentrator for the operation in various scenarios of advanced electrical networks, DER and Smart Grids. In addition to its versatile communication capabilities, it contains an embedded computer that provides processing capacity to implement distributed computing: capture and storage information, execution of algorithms and control of the installation among others. During the project, the current prototype of EB will be improved to be able to retrofit existing Secondary Substations, enhancing its assets control capacity.

The high penetration of RES, such as wind and solar, is impacting the operation of protection relays because this kind of generation behaves very different than conventional synchronous generation, due to their coupling through power electronic. Task 3.4 had the aim of studying the

impact of high RES penetration on feeder protection relays installed in MV primary substation and on fault passage indicators installed in MV secondary substations. In order to do this study, a benchmark MV distribution grid was defined and modelled in RTDS, using Hardware in the Loop (HiL), including high RES penetration with Photovoltaic (PV) and type 3 (DFIG) and 4 (FC) wind generators. Different test cases were defined, with different fault locations, fault types, fault resistances, load conditions, neutral connections, RES penetration level, Mv lines topology. Scripts were created to make automatic tests and reduce test time. All the cases were applied with and without Injection of negative-sequence current. The last version of the Spanish Grid Code was considered when defining the control of the mentioned converter-based generators.

The following functions were tested: phase overcurrent, ground overcurrent, phase / positive-sequence / negative-sequence / ungrounded directional, phase selector and frequency units. The main conclusions that were obtained are summarised below:

- Good operation of ungrounded directional overcurrent unit
- Lack of dependability of phase overcurrent units during phase-phase or three-phase faults.
- Erroneous operation of directional units (phase, positive-sequence, negative-sequence).
- Unreliable operation of phase selector based on currents.

During task 3.5, an analysis of the units that maloperated was performed and new algorithms were developed and implemented in the feeder relay and fault passage indicators. These new algorithms include:

- Use of distance units to increase the dependability during phase-phase and three-phase faults. The mentioned distance units included an improvement in the compensation of the apparent resistance, using appropriate line reactance polarizations.
- Use of a directional unit that combines positive-sequence voltages with phase currents or a dynamic combination of positive-sequence and negative-sequence directional units.
- Implementation of a phase-selector based on voltages.
- Voltage restrained units in the fault passage indicator

Matlab-Simulink modelling and simulations of type 3 and 4 wind generators were also done during task 3.5 in order to have further information about the RES behaviour.

During the second part of task T3.4 the testing of the feeder relay with the improved algorithms using RTDS was performed. A second phase selector based on superimposed voltages was developed and initially implemented in block diagram language RTDS Once debugged, it was translated to C-code to emulate its behaviour in a commercial protection relay. The C-code was implemented in a platform (PC Windows) and tested through the laboratory test bench These tests check algorithm behaviour using the mentioned grid model. Grounded and ungrounded systems were considered during the analysis, obtaining good results in all of cases.

On the other hand, in task 3.4, a WAMPAC scheme is proposed to improve the current protection system used in the distribution power system. The main objective of the developed protection scheme is to operate as backup protection of traditional schemes. The method, known as the "Zone IIA Method", is based on voltages and currents positive sequence phasors measurements provided by all PMUs installed in the boundary of the protected zone. A distribution grid was defined and several test were carried out to evaluate method performance.



Document: D3.7 Publishable report on physical architecture developments

Author: ZIV

Version: 2.0

Date: 01/03/2022

From test results it is concluded that the IIA Zone Method can protect against faults applied inside the protected line and protected zone. Furthermore, from tripping time values is also concluded that the method can act as backup of protection



1. INTRODUCTION

The main objective of WP3 is to design and develop new physical architecture bringing potential new solutions to the European market, which will allow the implementation of services currently unfeasible due to technical restrictions. To reach this objective, several solutions have been identified and developed within WP3. In this deliverable all the publishable results and conclusions on these new developments are described.

2. TASK 3.1. RESULTS AND CONCLUSIONS

Task 3.1 includes the design and development of a smart transformer (Transforma.Smart) and a Low Voltage Board (LVB- Addibo) and new functionality for the MV RTU (Web Services). IEC61439 has been followed for safe operation under normal and abnormal operation conditions.

This development will allow to take advantage of the available information and the communications channels used by meters, RTUs and other devices in an optimized way.

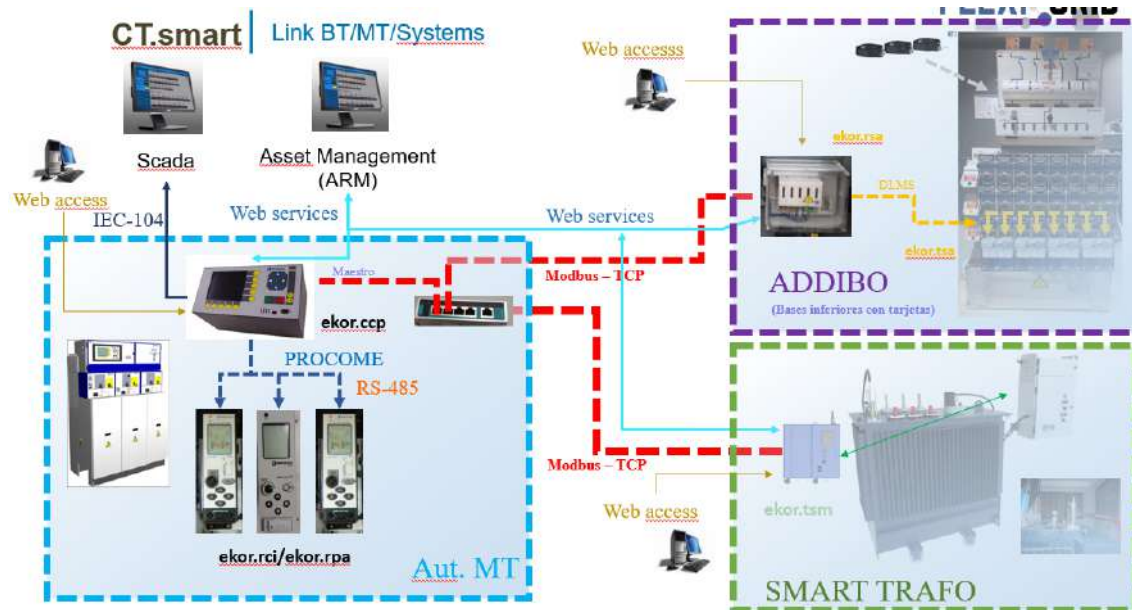


Figure 1: Secondary Substation of the future

New communication protocols will allow a better time of response, autonomous control and flexibility in the grid.

The development consists of:

- MV automation upgraded with new functionality (Webservices) integrated in the RTU. Based on the MV Secondary Substation automation it will be upgraded with the functionality of Webservices:
 - Initial Web Services of the project: (ready for the pilot)
 - i. Receiving the status of MV Automation SS.
 - ii. Reception of MV Automation events of the SS.
 - iii. Firmware update of the MV Automation RTU.
- MV automation upgraded with new digital densimeter installed in the cubicles sending to the control dispatch the SF6 pressure metering.
- New smart LVB that should follow IEC 61439 to achieve safe operation under normal operating conditions as well as under abnormal operation conditions. In addition to being arc fault tested according to IEC/TR 61641, any new designs should reduce the possibility of internal arc.

For this, the smart LV switchgear should be ready to relief connection point to a generator, preventing access to live parts during the bus bar connection. It should be ready for distribution bus bar extension with a coupling system design, that allows to do this operation safe, fast, and even with live voltage, keeping protection degree IP2X, reducing exposure to electrical hazards during bus bar extension and with reduced space, to minimize service interruption time.

As a preliminary step to the automated LVB, a monitored LVB is developed, with its control equipment. The new functionality and measures will allow better maintenance and control of the LV grid. The new equipment installed will be integrated with the communications of the SS with the idea of taking advantage of the potential installed.

As a part of the development, it will be a definition of:

- DDBB normalized and definition of primary and secondary signalling.
- Integration of primary signalling in MV automation RTU.
- Definition of secondary signalling and alarms for their integration in Webservices.
- New compact smart distribution transformer, with an On-Load Tap Changer (OLTC), able to regulate the voltage automatically to cope with the fluctuations generated by new loads and variable DG in the LV grid, while compensates voltages instabilities in the MV network.

Based on an electromechanical OLTC that can change the tap position automatically, and with load. The new smart distribution transformer can increase the LV network Hosting Capacity without the need of new infrastructure.

From the point of view of the smart transformer's control, a new control unit will be developed. Among all functions this control unit will have, the following can be cited:

- Control the smart transformer's step motor (OLTC)
- Transformer protection system by monitoring the magnitudes: T^a , Pressure and Oil level.
- Transmit to the control dispatch all low voltage measures among other signals (alarms, trips and tap status of the OLTC)
- Receive and set from the control dispatch:
 - Voltage set point for the smart transformer.
 - Tap change (Up/down)
 - Manual/automatic function

For the control equipment of the smart distribution transformer, there will be a definition of:

- Normalized Databases (DDBB) and definition of primary and secondary signalling.
- Integration of primary signalling in MV automation RTU
- Definition of secondary signalling and alarms for their integration in Webservices

The following figures show some of these developments for the Flexigrid Project.



Figure 2: Smart trafo designed for Flexigrid



Figure 3: Smart LVB

3. TASK 3.2. RESULTS AND CONCLUSIONS

Smart meter rollouts are happening all over the world, with utilities trying different approaches, technologies, and solutions to reach similar objectives including customer engagement, supply reliability and operational efficiencies.

DSOs designing their own smart meter is an option, but too expensive above all for small and medium DSOs, so only standard functionalities being available on the smart meter market are usually applied.

The selection of the communication technology is a critical point. Some parameters are usually considered for selection: reliability and robustness, cost, security, data protection and privacy, longevity of solution..., there is no one optimal communication technology for all and in many cases, there is a trend towards a hybrid solution.

In this sense, in this project a modular meter is proposed with more than one possibility, for communication with both the DSO and customer. Other design features that provide flexibility and technological durability has been also considered.

As result of this specification, a flexible smart meter has been developed and tested. This meter incorporates a special sealed holster designed to host a pluggable communication module which could be LTE Cat 1, Cat M1 or NBIoT for those scenarios where PLC communication is not an option or if redundance is needed.



Figure 4: Flexigrid meter

The meter has a PLC service node integrated over PLC Open Standards with ZIV technology: PRIME 1.4, Meters and More or G3 PLC.

Other features included in the design are:

- Robust automated meter reading (AMR)

- Energy measurement, load profiles, measurement profiles and Time of Use (TOU) features.
- Advances instantaneous measurements for LV grid operation.
- Integrated breaker for demand management or protection (temperature or overvoltage).
- Service Quality events (sags and swells, interruptions...)
- Remote configuration and firmware upgrade.
- Fraud detection features.
- Cybersecurity features.

On the other hand, the meter cannot be only seen as a billing meter, it is a sensor that, when installed in other points of the network, can offer even more valuable information. If we analyse the type of data exchanged between the data concentrators and the meters for the maintenance of the network, we can think about the applicability of automatic learning algorithms and as result, an algorithm to obtain the LV feeder identification of all the connected smart electricity meters has been developed. This algorithm helps network operators get a better insight on the LV network.

Mapping meters to feeders and phases is important for several reasons, including load balancing among feeders and phases, energy losses locating or punctual information about power interruptions.

The method designed in Flexigrid project is based on the mathematical formulation of the problem as an optimization model. It could easily be generalized to the phase identification problem. It is an iterative procedure for grid mapping in both a noiseless and several noisy (energy losses, missing loads, incorrectly assigned measurements...) cases. This procedure requires, on the one hand, the linear relaxation of the original problem with a strategy of progressive incorporation of measurement constraints for different time periods. On the other hand, it includes a prioritization strategy which is established to firstly identify the meters with the largest consumptions, taking into account the different solutions obtained in previous iterations, the analysis of the highest consumptions and, the progressive incorporation and implementation of a new set of valid inequalities (cuts) to the problem.

In T3.2 we have used real and synthetic smart meter datasets to develop an efficient procedure for feeder identification. We use a dataset of anonymized load measurements collected from customer meters connected to a set of feeders. Then, we have synthesized and simulated a network with a specific topology with the aim of evaluating the precision of the solutions obtained in terms of how exactly the pre-established network mapping becomes identified.

We have simulated a distribution network by assigning a set of actual meters to different artificial feeders or distribution lines in a pseudo random way.

The mathematical modeling of the feeder identification problem requires the following sets, parameters and variables.

- $T = \{1, \dots, |T|\}$: the set of time measurements;
- $I = \{1, \dots, |I|\}$: the set of indices for customers or meters;
- $J = \{1, \dots, |J|\}$: the set of indices for feeders or distribution lines to which the meters are connected.
- x_{ij} : the binary variable that shows if customer i is connected to line j .

- $x_{ij} = \begin{cases} 1 & \text{if customer } i \text{ is connected to feeder or line } j \\ 0 & \text{otherwise} \end{cases}$
- where $i \in I$ and $j \in J$.
- e_{jt} : it represents the errors or noise present in line j at time t . It is well known that in the distribution of power, part of it may be lost. e_{jt} arises due both to electricity losses and to certain unmetered loads on feeders such as street or traffic lights. On the other hand, new technologies and renewable energies make possible the existence of consumers who, at any given time, can contribute with energy to the system. Therefore, we consider that the e_{jt} variable can be either positive or negative.
- c_{it} : load (in kWh) of meter i at time t .
- T_{jt} : the total measurement (possibly erroneous) of line j at time t .

The objective of this distribution line mapping is to obtain, using an optimization model, the binary variable (x_{ij}) that assigns each customer to one of the distribution lines or feeders.

In order to evaluate the efficiency of the identification procedure, we have simulated a distribution network assigning the available meters to a set of fictitious feeders. Moreover, the total consumptions of the feeders, T_{jt} , have been created for the noiseless and noisy variants of the problem.

The identification procedure is an iterative procedure in which at each iteration a set of constraints per unit of time is added to the model, saving the corresponding obtained solution. Thus, at each iteration the model increases the number of constraints and does it up to a total number of constraints which in the last iteration is at most equal to the number of time measurements available. This iterative procedure does not only add the knapsack constraint but also the cuts linked to it, that are identified by using the error terms obtained previously.

The computational experience carried out on a real data set, provides results that support the efficiency of the proposed scheme. Further computational work with the algorithm in its latest version is yet necessary. In addition, to support the results, its behaviour should be tested with new real data collections, including the case of missing measurements or partial incorporation of known information, to further explore the performance of the proposed procedure.

4. TASK 3.3. RESULTS AND CONCLUSIONS

The purpose of Task 3.3 “Smartening of the grid architecture via Energy Box development” was to provide a valid smart gateway-concentrator to act as the middleware of FLEXIGRID architecture along the different demo sites involved.

This device has been developed by CIRCE, as an evolution of existing hardware solutions implemented in previous experiences in Smart Grid scenarios, but advanced technologies have been added within FLEXIGRID project in order to increase the visibility of the grid, and to provide both data acquisition and DER operation capabilities.

This task has been strongly linked to T5.1 “FLEXIGRID ICT architecture definition” and T5.2 “Protocols and standards, interoperability and CIM”, where the software architecture and communications along the different solutions of the project were defined and to T5.4 “FLEXIGRID Middleware and platform adaptation”, where the integration between FLEXIGRID platform and the Energy Box is dealt with. Therefore, specific information related to architecture and protocols should be consulted in deliverables from these tasks.

This Energy Box (EB) is part of the range of next-generation smart controllers. It integrates several of the most used communication technologies, resulting in a concentrator that reduces equipment and deployment costs. The microprocessor relies on a multi-core CPU architecture and non-blocking switching structure, providing a remarkable performance and industry-leading system capabilities.

Thus, the Energy Box provides a compact and embedded solution that permits controlling real smart devices. The key features of this system are:

- Compact and modern design.
- Fanless design that ensures quiet operation in small office spaces and living rooms.
- High level services and monitoring can be performed remotely whereas local services can be processed locally, which improves service quality, security and efficiency.
- Low power consumption.
- Debian based computer operating system.
- Reduced form factor and light weight.

The Energy Box hardware is formed by an *ad hoc* design to meet the communication capabilities and data processing required by the project developments, and a size and enclosure suitable for the limitations of the demo sites.

The Energy Box is the middleware between field devices and cloud platforms, adding interoperability functionalities between the two levels of communications.

Communications will be compatible with what was agreed in the Common Information Model developed in T5.2 “Protocols and standards, interoperability and CIM”, in terms of format and information exchanged to fulfill the needs of the platform and project developments.

Downward communications (with field devices) involve the connection between the auxiliary modules exposed in the hardware section, interfacing with the processor module that contains the main operative system and the main functionalities. The modules selected are meant to include some of the most used standards in the industry for wired solutions: serial

communications via Ethernet and RS-485/RS-232 modules; and wireless solutions: ZigBee, and Wi-Fi modules.

Some of the protocols have been programmed in their respective modules, specifically ZigBee and Wi-Fi protocols, but the rest of the protocols, like Modbus and the specific protocols of the rest of the equipment, have been programmed directly in the core module of the equipment.

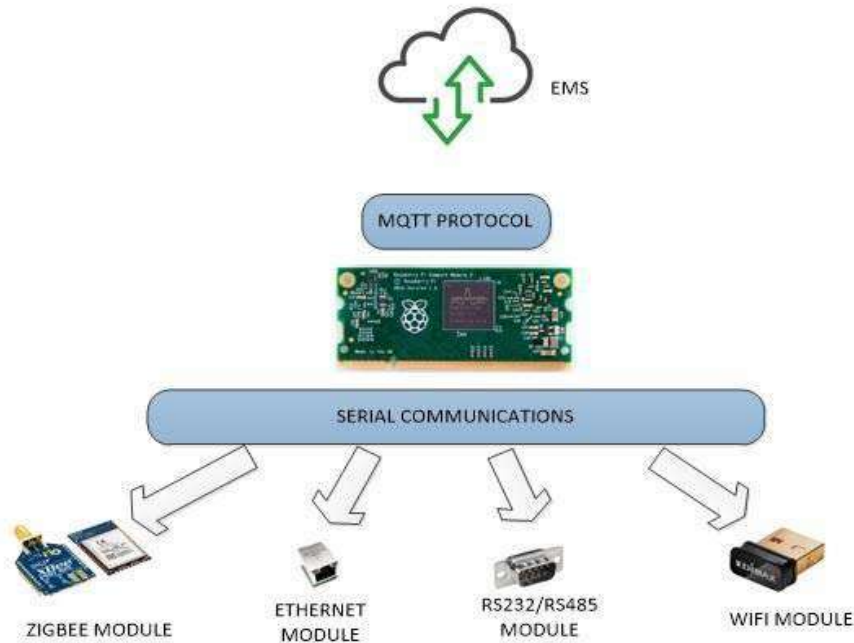


Figure 5.- Schematic of the downward (with field devices) and upward (with cloud platforms, like Energy Management Systems) communications of the EB.

For the cloud communications, the EB presents several possibilities, the most used ones are REST API and MQTT.

To sum up, the EB is also a modular software solution that provides communication capabilities, both upstream and downstream, with a wide variety of field devices supporting the main standard communication protocols, but also with different cloud platforms where advanced functionalities are implemented. Taking advantage of these advanced functionalities, it is possible to perform device control policies and provide flexibility and scalability for the control architecture.

These powerful, yet compact hardware solutions and their communications potentials, become strong assets towards a more sustainable future, providing the necessary infrastructure for the deployment of novel services and innovative business models.

5. TASK 3.4. RESULTS AND CONCLUSIONS

5.1 Grid Model

The benchmark grid is composed of a 55 kV HV external network and a 12 kV distribution grid. HV network is represented in RSCAD using a Thevenin equivalent. Two renewable technologies connected to distribution grid are considered to carry out the studies: PV and type 3 and 4 wind turbines. Overhead lines are used to connect renewable technologies to the distribution grid. Finally, an underground distribution grid topology is considered to perform the analysis.

The analysis of the behaviour of present protection systems is developed by using the Hardware in the Loop (HiL) configuration. Figure 6 shows the scheme used during the study:

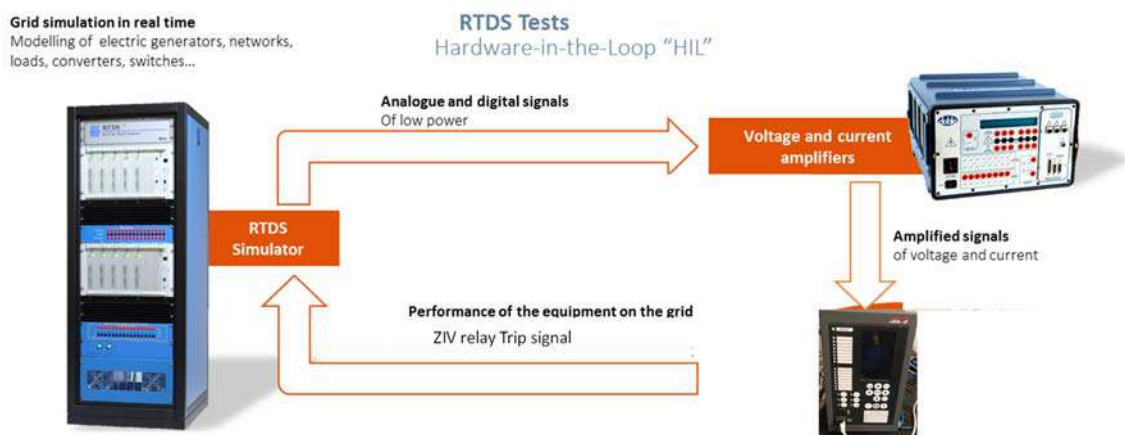


Figure 6. Hardware in the loop configuration

The distribution grid is modelled in RSCAD to perform the study. RSCAD is the tool used by RTDS to simulate the electric grid. From the RTDS simulation, current and voltage values to be measured by relay are generated and sent to the ZIV relay.

5.2 Scenarios and study cases

The benchmark distribution grid model described was used to evaluate protection relay performance under high penetration renewable scenarios. Several relay locations have been tested in order to define the most representative scenarios from the relay point of view. These scenarios are the following:

- Analysis of the performance of the relay when the renewable fault current contribution comes from distribution grid. In this case the following study cases have been considered:
 - Study case A: Evaluation of non-directional phase overcurrent (51P) and ungrounded directional elements (67Ns)
 - Study case B: Influence of capacitive currents in sensitive ground directional element behaviour (67Ns)
 - Study case C: Influence of ground connection of HV grid in non-directional phase overcurrent (51P) and ungrounded directional elements (67Ns)
 - Study case D: Influence of distribution load variation in non-directional phase overcurrent element (51P)

- Study case E: Influence of renewable generation in frequency elements of protection relay
- Study case F: Influence of negative current injection based on new grid code
- Analysis of the performance of the relay when the renewable fault current contribution comes from Low voltage grid
- Analysis of the performance of the relay when the renewable fault current contribution comes from High voltage grid

For analysing the behaviour of each study case, the following fault types were carried out:

- Line to ground fault: LA-G
- Line to line fault: LAB
- Line to line to ground fault: LAB-G
- Line to line to line fault: LABC

Furthermore, two different renewable penetration levels were used in order to cover a wider view for the results:

- Rated power=3 MW
- Rated power=11 MW

5.3 Main conclusions from the test results performed on the conventional feeder relay

From tests the following conclusions were obtained:

- Fault current contribution from renewable generators based on power electronics is limited during fault conditions. Therefore, it might be necessary to enhance the algorithm to detect fault current magnitude with the aim of detecting pick-up current. Furthermore, new protection schemes not based on overcurrent elements could be needed to avoid coordination mistakes.
- Operational problems in distribution grid can appear due to the limited renewable fault current contribution. If the relay located at feeder does not detect the fault but the renewable resource detects it and disconnect, the fault will not be cleared, and the renewable will try to reconnect under fault conditions. It could damage the renewable resource and it could lead to the owner of renewable resource not being able to deliver the rated power.
- The unpredictable nature of generation units and demand can involve coordination problems. Settings definition of overcurrent protection is an important task to be redefined.
- Present settings criteria used by electrical companies could not be appropriate in scenarios with high level renewable penetration. When there is a fault in the electric grid, the renewable generation will be disconnected due to grid codes before the relay operation.
- Directional protections are needed in the new grid configuration because the power can flow in both directions. The criteria used for directional detection to set the angle is commonly based on line impedance, but it must be reviewed to take into account the influence of renewable resources. The criteria used to detect directionality varies between the different relay manufacturer and depending on the selected criteria

(positive sequence, negative sequence, etc..) the relay could not detect the fault direction correctly due to the waveform of the current injected by the PE based renewable sources.

- Traditional phase fault selector element has a wrong operation when unbalanced faults are present in the electric grid and negative sequence current is not injected. The tests carried out shows a better phase fault selector operation by using negative sequence current injection in power converters used to connect these generators.
- In the distribution grid, loads are located close to the generation points, and it was expected that such loads could help to phase fault selector to find out a line to line fault. However, results from the test show that in the case of FCWT, the phase fault selector is not able to identify correctly the phases involved.

5.4 Grid code and negative-sequence current injection

The Spanish grid code published in July 2020 [1], defined new requirements for fast fault current injection under unbalanced faults. To evaluate the influence of these requirements in the protection relay behavior, they have been implemented in power electronics used by PV and type 4 wind turbines RSCAD models. From new grid code analysis, two strategies for defining the priority of positive and negative sequence current injection are considered for the current limits of the equipment. These strategies allow to evaluate the behavior of the current protection system when an unbalanced fault is applied. From test results, it is concluded that phase fault selector operation improves the relay behavior in line-to-line faults for the analyzed algorithm. However, for the other fault types, the behavior is still wrong. Therefore, a new algorithm is needed to work with this new scenario.

5.5 Solutions developed

The following sections describe three solutions proposed to be applied in the distribution grid:

- 1) Phase selector based on superimposed voltages
- 2) Phase selector based on sequence voltages plus distance units with improved compensation of the apparent fault resistance plus improved directional units
- 3) WAMPAC system based on μ PMUs located along the distribution grid.

5.5.1 Solution 1: Phase selector based on superimposed voltages

A phase selector based on superimposed voltages was implemented. Superimposed quantities are methods fast and reliable that considers the information available during the initial transient period after fault inception. The proposed phase fault selector algorithm is initially implemented in block diagram language RTDS to identify the phases involved in the fault (AG, BG, CG, AB, BC, ABG, BCG, CAG or ABC). The general diagram of the algorithm is shown in Figure 7.

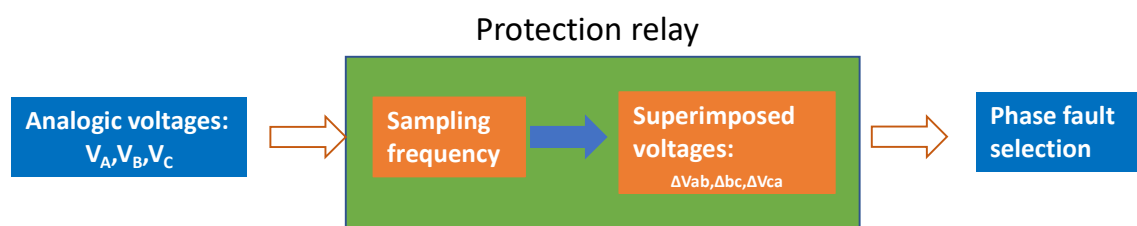


Figure 7. General diagram of the algorithm.

After debugging the algorithm, it was translated to C-code to emulate its behaviour in a real protection relay. The C-code is implemented in a platform (PC Windows) and it was tested through the laboratory test bench. Several faults have been applied and it is concluded that the new algorithm has operated correctly for all test cases.

5.5.2 Solution 2: Phase selector based on sequence voltages & Distance Unit with Improved Apparent Fault Resistance Compensation

Table 7 shows the operation of a phase selector based on currents and of a classical distance protection when exposed to fault records from both RTDS PV and wind type 4 models with negative sequence current suppression and to Simulink type 3 and 4 WT models with negative sequence current injection. It can be checked that there are cases where the operation is wrong.

The new solutions, including the phase selector based on sequence voltages and the distance units with improved apparent fault resistance compensation, implemented in a ZIV IRF prototype feeder relay, were tested with the mentioned fault records giving good results.

They were also tested with oscillograph registers taken from final RTDS PV source model with negative sequence current injection Strategy B and RTDS Type III WT model. Faults were simulated at 50% of Line 3 of the Benchmark Model varying source type. The results are shown in table 1.

Unit	Type III WT		PV	
	PH_SEL	21	21	PH_SEL
AG	✓	✗	✓	✓
AB	✗	✗	✗	✓
ABG	✗	✗	✗	✗
ABC	✗	✗	✗	✗

Table 1 Typical Current Based Faulted Phase Selector and Classical 21 Unit Results

Unit	Type III WT		PV	
	PH_SEL	Fault resistance R=0.1 Ω	Fault resistance R=0.1Ω	PH_SEL
AG	✓	21	21	✓
AB	✓	✓	✓	✓
ABG	✓	✓	✓	✓
ABC	✓	✓	✓	✓

Table 2 Voltage Based Faulted Phase Selector and 21 Unit with Apparent Fault Resistance Compensation Results

5.5.3 Solution 3: Protection scheme based on wide area protection system

Wide area protection scheme which is typically more oriented to transmission grids is adapted to be used in the distribution power system. The main objective of such protection scheme is to operate as backup protection of traditional schemes. The implemented system is based on the use of the Integrated Impedance Angle (IIA) [2] [3] along with the theory of Virtual Bus [4]. The method, known as “Zone IIA Method”, is based on voltages and currents positive sequence phasors measurements provided by all PMUs installed in the boundary of the protected zone.

A distribution grid was defined and several test were carried out to evaluate method performance. From test results it is concluded that the IIA Zone Method can protect against faults applied inside the protected line and protected zone. Furthermore, from tripping time values is also concluded that the method can act as backup of protection

6. TASK 3.5. RESULTS AND CONCLUSIONS

6.1 Behaviour of type 4 wind and PV generators

As described in T3.4 summary, the behaviour of type 4 wind generator during fault conditions solely depends on the grid code. The last version of the Spanish Grid Code has been described

6.2 Behaviour of type 3 wind generator

The behaviour of type 3 wind generator depends on both the control system and the physics of the asynchronous machine:

- Due to the principle of flux conservation DC fluxes are generated in both stator and rotor
- AC fluxes in both stator and rotor
- AC and DC currents in stator and rotor
- It behaves as a pure asynchronous machine when crowbar operates

6.3 Sequence networks with converter-based generation

- The voltage sources are replaced by current sources, however a current source can be replaced by a voltage source in series with a variable impedance.
- Positive-sequence network: the pure fault positive-sequence source impedance may have angles higher than 90° due to the limitation of the current required by the power electronics; this creates a high non-homogeneity of the pure fault positive-sequence network
- Negative-sequence network: some converter-based generators do not inject negative-sequence current
- Zero-sequence network: although the converters are isolated from ground the transformer that connects to the network is normally Dyn, so it contributes with zero-sequence current

The problems described with the positive and negative-sequence networks lead to wrong operations of phase selectors based on currents and on distance protection line reactance conventional polarizations

6.4 New developments implemented on feeder relay IRF model and on fault passage indicator TCA model

6.4.1 Phase selector based on voltages

The use of the sequence networks for AG, AB and ABG faults have been taken into account to obtain the phase shifts between V_1 , V_2 and V_0 . Based on this relationship, the following angular sectors for the angle between V_2 and V_1 and for the angle between V_2 and V_0 have been proposed

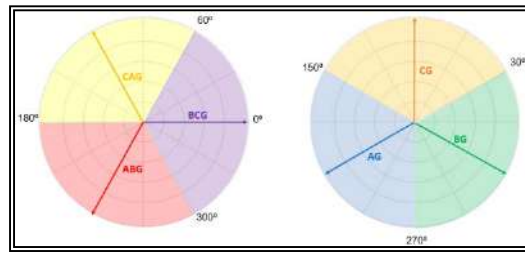


Figure 8 ϕ_{V1} Angular zones for faulted phase selector.

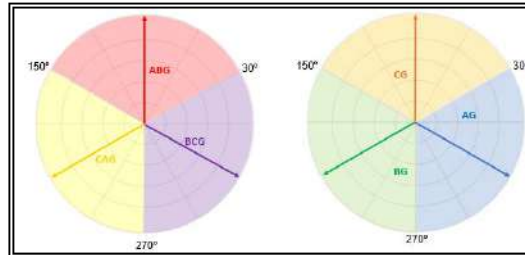


Figure 9 ϕ_{V0} Angular relationships for faulted phase selection.

6.4.2 Distance protection with improved compensation of the apparent fault resistance

Given the issues found with the use of protection units based solely on current, distance protection is added to equipment design for distribution grid protection. Phase distance units, based on the impedance measurement, are more dependable than phase overcurrent units when the short circuit current is closer or even lower than the load current, because they are independent from the short circuit current if it is above a minimum threshold.

However, adequations to currently used distance units need to be done to adapt to the changing impedance that RES and DER might represent to the system. More specifically, the reactance line polarization is reviewed to compensate the effect of the apparent fault resistance.

In general, for any type of fault, the following expression can be used:

$$V_r = I_r \cdot Z_{1LF} + I_F \cdot R_F \cdot k,$$

where V_r and I_r are local voltage and current used for each fault type, Z_{1LF} is line impedances up to the fault location, I_F is the current that circulates through the fault resistance and k a constant ($k=1$ for single phase faults and $K=1/2$ for multi-phase faults). Dividing all factors by I_r , impedance seen by distance units is $Z_r = Z_{1LF} + \frac{I_F}{I_r} \cdot R_F \cdot k$.

As seen in Figure 10, the impedance see by the relay is not the positive sequence impedance up to the fault location, but a new factor is added, $\frac{I_F}{I_r} \cdot R_F \cdot k$, called apparent fault resistance.

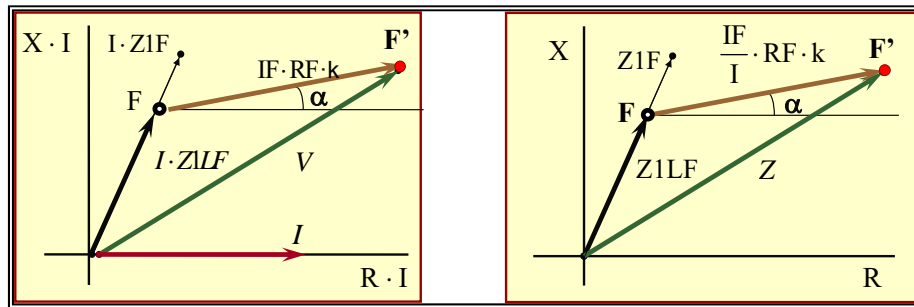


Figure 10 Impedance seen by relays on a) voltage diagrams $(R \cdot I - X \cdot I)^1$, and b) impedance diagrams $(R - X)$.

Apparent fault resistance shows α angle due to the phase difference between I_r and I_f , which mainly depends on two factors, load and system non-homogeneity. Following section describes the method developed to compensate both effects.

Different polarization methods are used depending on the fault type and negative-sequence current injection; a compensation of the system non-homogeneity is also done using the local source, line and remote source impedances. The local source impedance is calculated in real time with the voltage and current measurements (zero, negative or pure fault positive-sequence depending on the type of fault). The polarization phasors are taken from the pure fault sequence connections from the different type of faults.

6.4.3 Directional units

Positive-sequence directional unit (67P): behaves correctly except when the crowbar of the type 3 wind generator operates. The crowbar operation can be detected with the I_2/I_1 ratio.

Negative-sequence directional unit (67Q): behaves correctly only when the generator injects reactive negative-sequence current.

Neutral / ground directional unit (67N): behaves correctly when the fault is grounded

67P/PH (67P21): uses the positive-sequence voltage and the phase currents. It behaves correctly for any fault condition.

Based on the results, the use of 67P/PH was implemented. It was also implemented the change from 67P to 67Q when a crowbar activation was detected.

6.4.4 Voltage Dependent Overcurrent Units (implemented on TCA fault passage indicator)

Voltage dependent phase overcurrent units are more dependable than standard phase overcurrent units when the short circuit current is closer or even lower than the load current. The higher dependability is provided by the decrease of the pick-up value when a voltage decrease is detected. There are two types of units available in the prototype:

- **Voltage controlled units:** the phase overcurrent units only pick-up if undervoltage units activate. As the sensibility problems occur during ungrounded faults, the undervoltage units operate with phase-phase voltage as shown in .

¹ The current "I" represents local current seen by the relay I_r .

Phase Current	Control Voltage (Phase Sequence ABC)	Control Voltage (Phase Sequence ACB)
IA	UAB	UAC
IB	UBC	UBA
IC	UCA	UCB

Table 3 Phase current and control voltages.

- **Voltage restraint units:** the pick-up value is dependent on the phase-phase voltage value, following the characteristic shown in Figure 11.

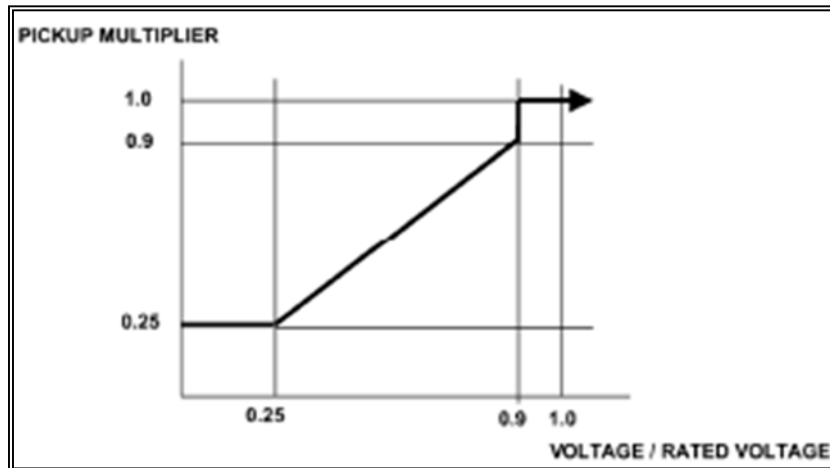


Figure 11 Pick-up value vs Measured phase-phase voltage

6.5 Additional SIMULINK model

Since distance protection units are implemented in the MV feeder relay, a higher voltage level grid model was also used to apply additional testing, taking in account remote infeed effect, which is not present in certain fault locations at the distribution level. Additional models of the two wind turbine types were developed for results comparison and for a deeper understanding of the internal control and protection features of the wind turbines impacting fault response. Models developed are based on the so-called Detailed Models in MATLAB Simulink®, as shown in Figure 12. The difference between the DFIG and FCWT models lies on the Wind Farm block shown in blue.

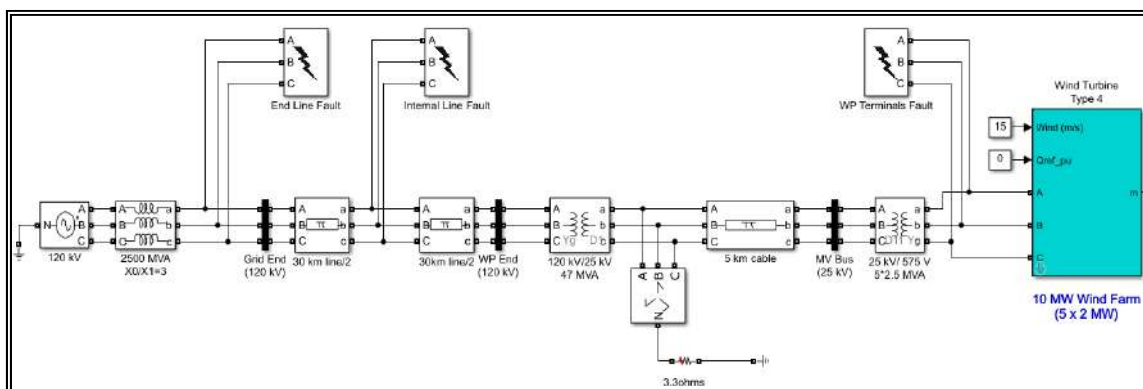


Figure 12 Test line model

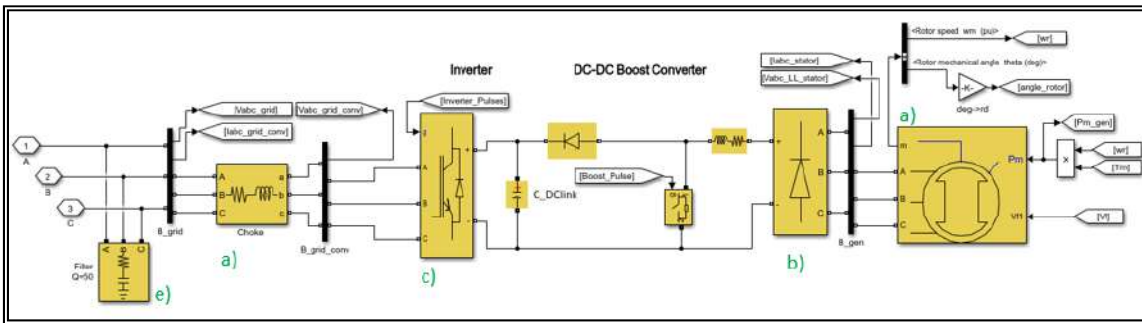


Figure 13 Full converter Wind turbine Model

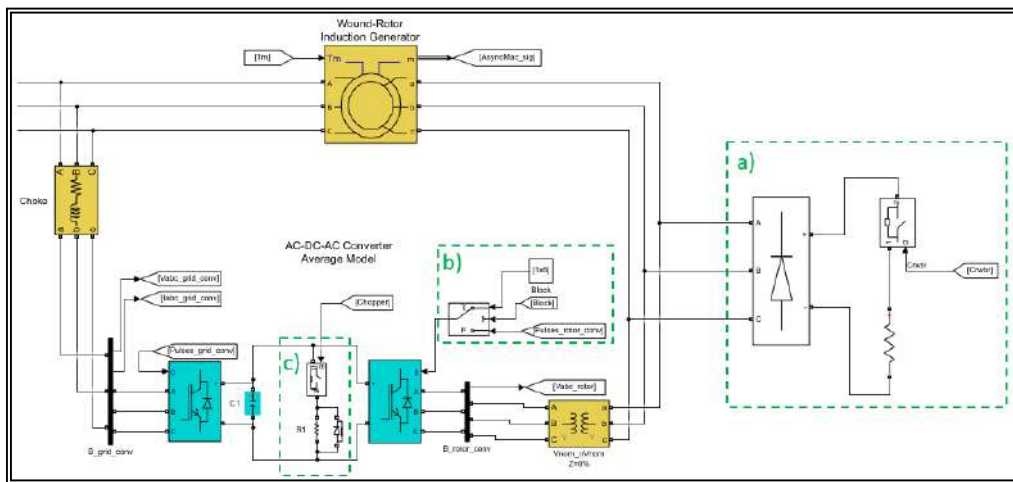


Figure 14 DFIG Detailed Model with RSC Protection

6.6 Testing of algorithm improvements with RTDS model results

As it was shown in tables 1 and 2, corresponding to task T3.4, the results of the phase selector and distance protection during RTDS testing were correct. Two examples are shown below:

On Figure 15 the AB fault presented in D3.4 under scenario 9.1, study case A is shown, in which the contribution from a FCWT with I2 suppression was recorded.

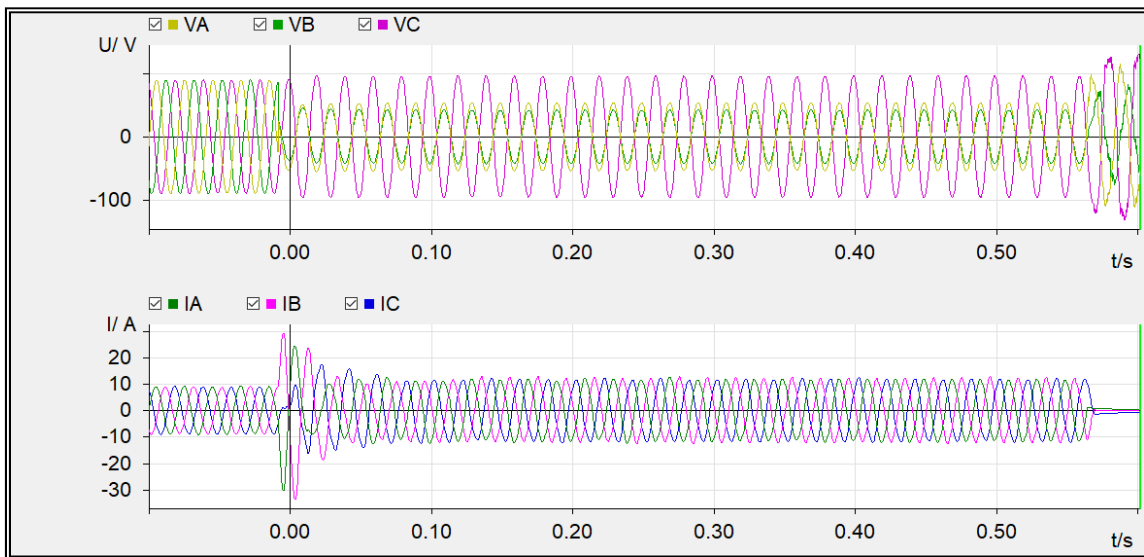


Figure 15 Scenario 9.1; Case A; FCWT with I2 suppression contribution

Following results were obtained for the phase selector, in which the lack of I2 makes the fault look like a three-phase fault from the current point of view as shown in Figure 16.

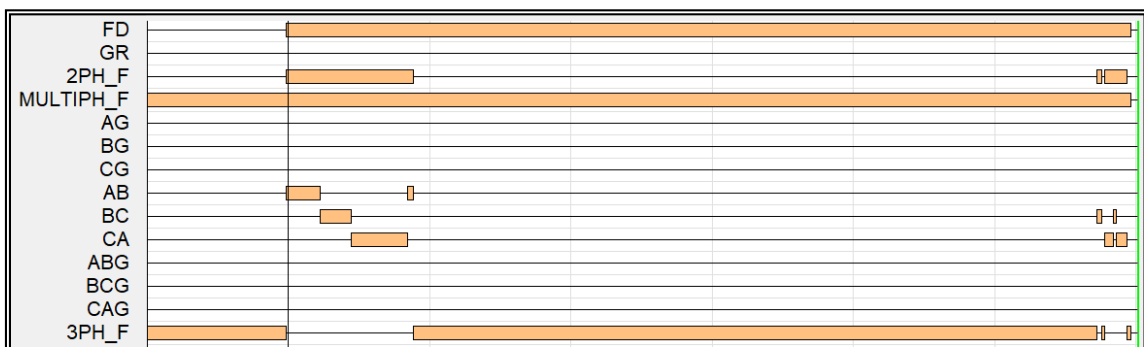


Figure 16 Current based faulted phase selection for AB fault under FCWT with I2 suppression contribution.

However, prototype results show an immediate correct identification of the faulted phase as shown in Figure 17.

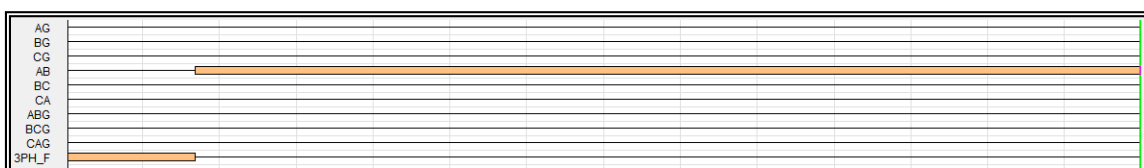


Figure 17 Voltage based faulted phase selection for AB fault under FCWT with I2 suppression contribution.

Faulted phase selector was also tested under DFIG contribution for an AB fault, showed below on Figure 18.

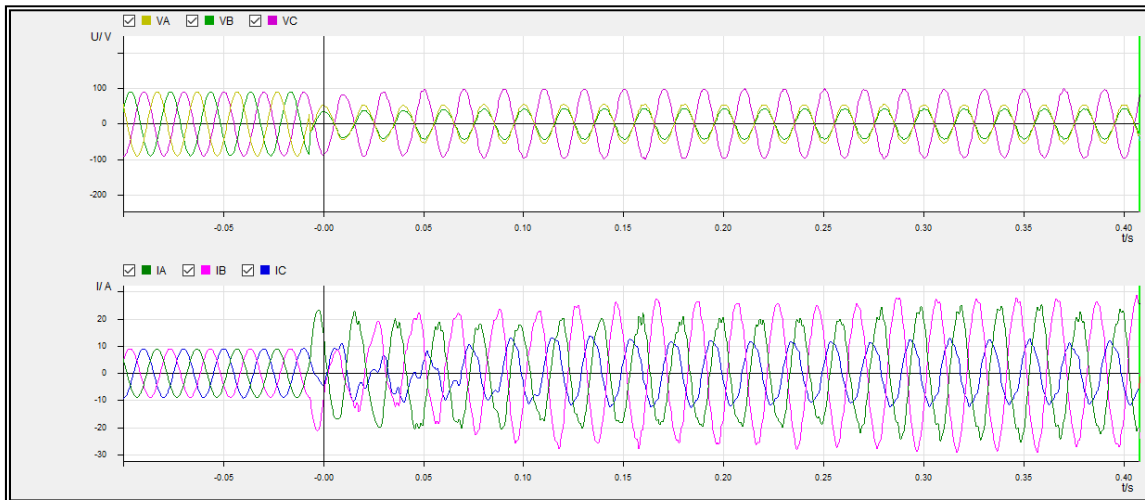


Figure 18 DFIG contribution to AB fault.

For which current based phase selector fails to identify correct phase due to abnormal current pattern:

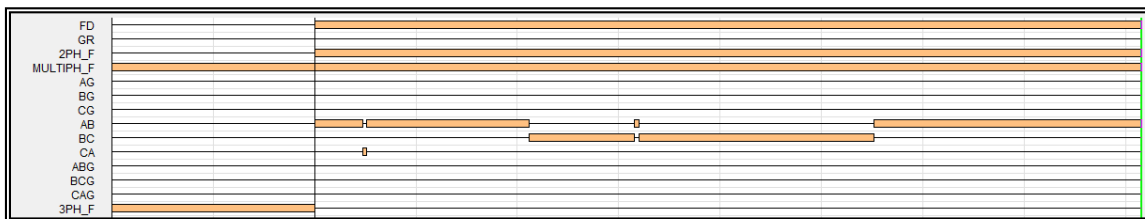


Figure 19 Faulted phase selection of current based selector under DFIG contribution.

While voltage-based selector operates correctly:

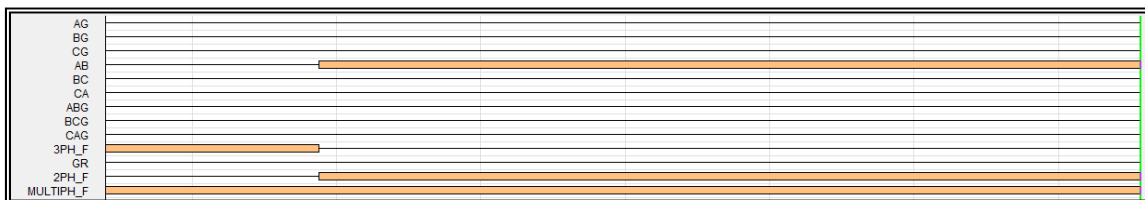


Figure 20 Faulted phase selection of voltage based selector under DFIG contribution.

The impact of compensating the local source angle is shown under impedance locus simulation for an AG fault feed by the PV model, in which 1.5 Ohms of fault resistance were added,

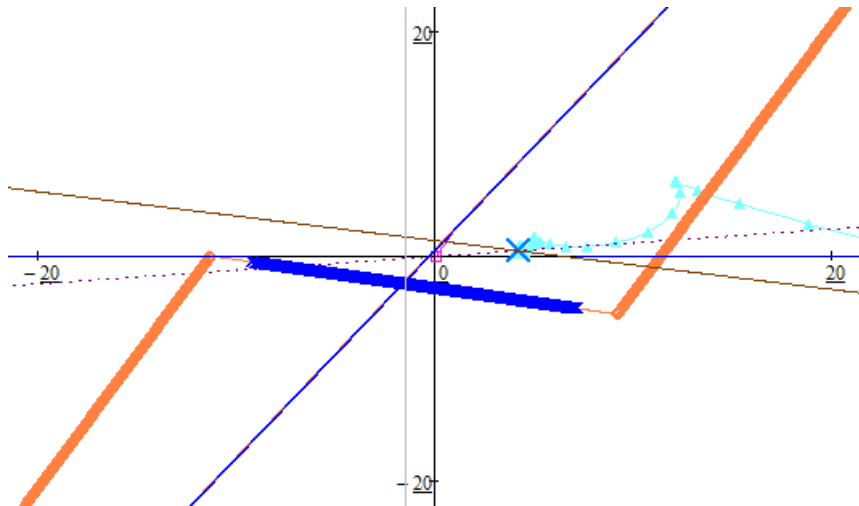


Figure 21 Quadrilateral distance characteristic for a AG fault feed by Type III model.

On , quadrilateral distance characteristic is shown. Directional line is shown in bold blue, while resistive limiters are shown in orange. Blue line represents reactance line, calculated using I2 as polarization phasor. The angle of the reactance line, in this case, due to the varying local source impedance, does not match with the angle of the apparent fault resistance shown in brown. The new polarization phasor that considers a real time calculation of the local source impedance shows in , that the reactance line follows more closely the angle of the apparent resistance, covering the fault impedance locus into the operating characteristic.

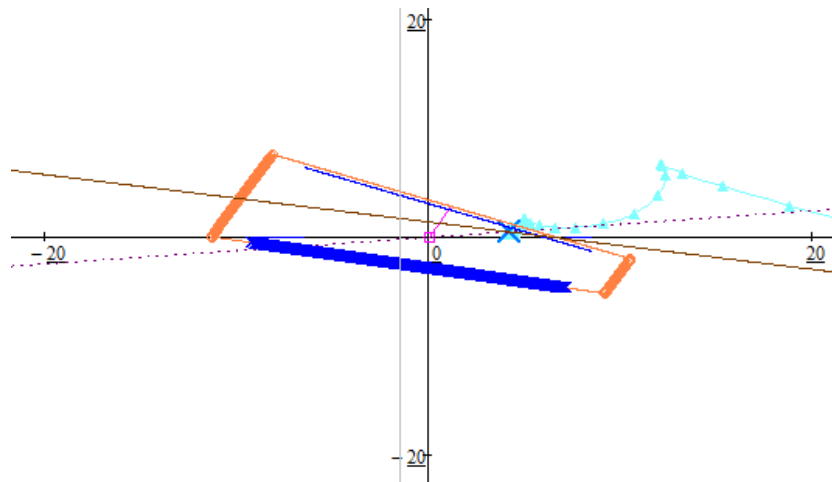


Figure 22 Quadrilateral distance characteristic for a AG fault feed by Type III model. Compensated.

6.7 Testing of algorithms improvements on SIMULINK model results

Fault records based on Simulink model for DFIG and FCWT were extracted, and algorithm operation simulated. In Table 4 the results for FCWT model, with I2 injection at 50% of the line and different faults and fault resistance are shown for the protection units previously analyzed.

Angles that make the protection function work properly with typical settings are highlighted in green. The ones causing a malfunction are shown in red. In yellow are the ones that fall into the right angular zone but does not stabilize.

RF/RG (Ω)	Falta	67P	67 Δ P	67Q	ϕ_{I1}	ϕ_{I0}	ϕ_{V1}	ϕ_{V0}
0	AG	47°	121°	93°	28°	-9°	180°	-3°
0	AB	48°	122°	84°	92°	N/A	240°	N/A
0	ABG	48°	102°	80°	83°	127°	240°	120°
10	AG	52°	131°	86°	37°	-3°	189°	2°
10	AB	53°	129°	85°	97°	N/A	247°	N/A
10	ABG	75°	126°	87°	72°	87°	240°	87°
50	BG	61°	160°	86°	170°	228°	-20°	238°
50	CG	62°	158°	86°	289°	108°	98°	118°
50	BCG	76°	142°	88°	190°	290°	0°	290°
50	CAG	75°	141°	88°	300°	170°	120°	168°

Table 4 Results for FCWT contribution.

Since the Type IV model is adapted to comply with LVRT requirements, 67Q work properly, which would not happen in presence of legacy WTs not complying with the most actual grid codes. 67 Δ P is not trustable, as expected from the impedance angle analysis and the angular relationships between sequence current is distorted due to the WT injection. However, voltage angular relationships remain trustable.

In Table 5 the results for Type III generation for a fault at 50% of the line are shown.

RF/RG (Ω)	Falta	67P	67 Δ P	67Q	ϕ_{I1}	ϕ_{I0}	ϕ_{V1}	ϕ_{V0}
0	AG	75°	158°	88°	59°	-4°	180°	-4°
0	AB	61°	166°	83°	133°	N/A	240°	N/A
0	ABG	79°	132°	83°	102°	119°	240°	115°
50	AG	53°	165°	92°	64°	-8°	218°	-3°
50	BG	49°	162°	91°	183°	234°	-23°	237°
50	CG	49°	162°	91°	183°	234°	-23°	237°
50	ABG	110°	164°	86°	98°	49°	240°	49°
50	BCG	110°	164°	86°	220°	-40°	0°	288°
50	CAG	110°	164°	86°	338°	170°	120°	168°

Table 5 Results for Type III Generation

In both cases, Type III and IV, phase selector angle ϕ_{I1} shows not to be trustable, since as it was seen before, pure fault positive sequence impedance is impacted by the control injection requirements. However, both voltage-based angles work correctly, despite of the fault resistance, whose impact stays within expected limits. Regarding the directional units, it is important to mention that zero sequence directional is another trustable element that can be used since the transformer supplies enough I0 to the fault.

For results shown in Table 5, an intermittent activation of the crowbar was observed, but it allowed the control to inject power accordingly to LVRT requirements. However, further simulations made, in which crowbar was forced to stay connected during the entire duration of the fault modified positive sequence angle since short circuiting the rotor makes the DFIG generator work as an induction machine, absorbing reactive power. This effect modifies the angle of the positive-sequence local source impedance, as shown in Table 6, in which both fault

and pure fault positive sequence directional units fail (67P, 67ΔP). Regarding pure fault positive sequence directional unit, it is very close to indicate an external fault as the default setting is 120°.

RF/RG (Ω)	Faluta	67P	67ΔP	67Q	ϕ_{I1}	ϕ_{I0}	ϕ_{V1}	ϕ_{V0}
0	AG	-50°	-165°	68°	116°	12°	178°	-8°
0	AB	-50°	-169°	69°	170°	N/A	240°	N/A
0	ABG	-50°	-180°	66°	167°	142°	240°	120°

Table 6 Results for Type III with Crowbar active.

6.7.1 Apparent fault resistance compensation.

In Table 7, it is shown how the angular difference between the proposed compensated polarization phasor for each fault and the current flowing through the fault resistance is close to zero. However, if phase or phase to phase current (depending on fault type) are used, the angle might not be close to zero. Neither with pure fault phase or phase to phase currents. In this case, I₀ will be used as a polarization phasor, since it remains a trustable polarization phasor in this case, as shown in theoretical analysis.

DFIG Crowbar Activation	Fault Type	RF (Ω)	Fpol vs IF angle difference (°)
Active	AG	50	-1,5
Active	AG	0	-1,2
Active	ABG	50	-1,1
Active	ABG	0	-1,3
Active	AB	50	-1,2
Active	AB	0	-1,3
Active	ABC	0	-1,2
No Active	AG	50	-1,5
No Active	AG	0	-0,6
No Active	ABG	50	-1,3
No Active	ABG	0	-1,5
No Active	AB	50	-1,1
No Active	AB	0	-1,5
No Active	ABC	0	-1,2

FCWT Fault Type	RF (Ω)	Fpol vs IF angle difference (°)
AG	50	-1,6
AG	0	-1,4
ABG	50	-1,3
ABG	0	-1,4
AB	50	-0,9
AB	0	-1,6
ABC	50	2,2
ABC	0	-0,6

Table 7 Polarization angle compensation for a) DFIG, b) FCWT

7. CONCLUSIONS

As conclusions, in WP3 the following specific objectives have been achieved:

- To develop the next generation of Secondary Substation for MV/LV grids
- To increase the functions and intelligence of the grid meters
- Upgrade the features of the Energy Box
- Improve grid protections capacities.
- Test the protections in a simulated environment

The next step is to install these solutions in the demo sites and monitor their behaviour to incorporate the improvements that are necessary to complete the objectives of the project.